Characterization of Resident Space Object States Using Functional Data Analysis

Thomas Kelecy and Emily Lambert
L3Harris, Colorado Springs, CO USA

Sufyaan Akram and John Paffett
Applied Space Solutions Limited, Hampshire, UK

ABSTRACT

To date, most characterization techniques (e.g. using photometric light curves) take place using time and frequency domain analyses of data samples generally lacking in the complete information content needed for unambiguous characterization of non-resolved Resident Space Objects (RSOs). In this paper, we examine the information content of multiple measurement types using information theoretic and functional data analysis (FDA) approaches which have shown promise in characterizing the physical and dynamic attributes of space objects from non-resolved observations [1, 2]. With limited data and information it may still be valuable to understand whether the "state" of an RSO is: (a) active (operational), (b) passive (debris), (c) dormant (a potential threat acting passive), or (4) transitionary between any of 2 of the a-c states. Representative use cases are established and the information content is examined in a probabilistic context for a set of simulated astrometric, photometric, Long Wave Infra-red (LWIR) and Radio Frequency (RF) observations for a diverse set of object shapes, sizes and dynamics representative of states a-d are used to demonstrate the application and value of FDA. The results confirm the value of these approaches by correctly categorizing independent sets of measurements and quantifying the likelihood of a given combination of observation types as being associated with a specific object. The value and information contribution of each observation type to the characterization probability is assessed.

Keywords: Satellite State Characterization; Probabilistic Analysis; Information Theory; Classification.

1. INTRODUCTION

A Resident Space Object (RSO) can be observed from Earth or Space-based sensors using one or more sensor modalities depending on the physical attribute of interest. Orbital time history of the RSO is inferred from astrometric data derived from optical images collected in the visible domain. Photometric signatures are the time histories of visible light reflected from Earth orbiting space objects as observed by a ground or space-based optical sensors. They are a function of the relative geometry between the Sun-object-observer, size, shape, material composition and attitude dynamics. The attitude dynamics are coupled to the orbital dynamics – e.g. through area-to-mass ratio variations which affect solar radiation pressure and drag – and hence, through dynamic mismodeling, affects the ability to accurately track and predict the orbital motion of un-controlled space objects. Measurements taken in the thermal wavelength domain also characterize the state of an RSO based on whether or not it has active sensors or subsystems, and the emitted radiation is also a function of the environment and the material composition of the object. Radio Frequency (RF) signals emitted from an RSO indicate active communications are taking place. The combination of these observed modalities enable us to unambiguously infer physical attributes that point towards the RSO being in one of four states:

a) Active – an operation state with payloads and systems enabling stable dynamics for orbit and attitude control
b) Passive – No active orbit or attitude control, and no active payloads
c) Dormant – The RSO has attributes indicative of it being Passive but occasionally exhibits attributes of an Active RSO
d) Transitioning – A state indicative of a transition between any a-c states, such as active control to non-controlled which could happen if an anomaly were to occur on an active satellite

The challenge is that for, any single measurement type, the signatures from one or more detected objects may be ambiguous and not afford any unique combination of physical attributes enabling clear association of the measurements to a specific RSO. How do we know which sets of signatures are associated with the same object? Or to a different object? The analysis presented here approaches these questions from an information content perspective.

Accurate and appropriate correlation of signatures through fusion of multiple measurement types lead to more accurate shape and attitude retrieval, as well as more accurate physical and dynamic characterization to support improved object identification and track custody.

In space surveillance, Earth-orbiting objects that are too small or too far away from an optical sensor cannot be spatially resolved in the observed images. Thus, un-resolved measurement time-histories of the tracking, visible photometric signatures, emissivity-area-product and RF emissions that collected from ground and space-based sensors are now being used to extract stability, size, shape, and attitude information about objects being observed to support Space Situational Awareness (SSA). The measurements are each a function of the orbital and attitude dynamics, size, shape, reflective characteristics and the space environment of the object, in addition to the phase angle defined by the Sun-object-observer geometry and range between the object and observer. Though it is difficult to separate these physical attributes unambiguously using any single measurement type, in the absence of a priori information as is the case for orbital debris, it can be assumed that each object should have combined characteristics that are unique to the individual object. Furthermore, each measurement type extracts unique information on the physical and dynamic attributes that is independent of the other measurement types.

Topics this paper will address are: (1) If two or more sets of signatures are collected from one or more sensor locations, and no a priori association between them is known, can one associate the content of the signatures to a quantifiable degree of certainty? (2) If one or more sets of signatures are collected from one or more sensor locations that are known to associate with a common object, how many observations are needed to unambiguously characterize the size, shape, periodicity and attitude information content of the object data? This work establishes a set of scenarios whereby simulated observations that encompass size, shape attitude and reflective characteristics are generated for RSO's having unique attributes of (a) active, (b) passive, (c) dormant or (d) transitionary RSOs. Then information theoretic algorithms are applied to assess the information content. The results demonstrate the value of associating multiple signatures and data types, and enabling space surveillance analysts to determine when sufficient data have been collected to unambiguously determine stability, size, shape and attitude. These attributes are directly related to the attitude and orbital dynamics and benefit the tracking and prediction of all space objects.

The paper is organized as follows. Section 2 describes the problem formulation. Section 3 describes the simulation setup and the generation of the sample observational data. Section 4 describes the functional approach where each measurement type is modelled as a series expansion that can be analyzed for information content. In section 5 the analysis for determining the state characteristics using various combinations of the measurement types is presented. Section 6 provides conclusions on the viability of using the proposed techniques to classify object attributes.

2. PROBLEM STATEMENT AND ASSUMPTIONS

The state of an RSO can be inferred through fusion of a variety of observational phenomenologies that infer different physical attributes representative of a given state. The hypothesis examined in this work seeks to identify which measurement combinations reduce ambiguities that might be inherent in any one or more measurement types. Optical systems with cameras and photometric sensors are designed to collect reflected photons from an RSO whether it is orbiting the Earth or on a Trans-Lunar trajectory and might not distinguish between an uncontrolled piece of debris and a dormant RSO. The visible photometric data can infer attitude dynamic stability indicative of a controlled vehicle, or in the case of an uncontrolled satellite, periodic spin (uncontrolled tumbling). The tracking data, typically in the form of topocentric Right Ascension (RA) and Declination (Dec) angles, along with the tracking rates, can infer dynamics associated with active satellites such as maneuvers. Similarly, Long Wave Intra-Red (LWIR) sensors collect thermal emissions in terms of measured flux over a band of wavelengths can be examined for indications of active sensors and/or thermal control in the form of temperature signatures that might be higher than those of defunct satellites or orbital debris. Lastly, active (or dormant) satellites will rely on at least periodic communications with ground stations for down-link of health and status and payload transmissions or uplink of new command sequences or parameters to support operations. Detection of Radio Frequency (RF) signals are indicative of an active RSO.

Each of the measurement signatures examined is a function of time varying features of the RSO. For example, it is well known that ageing effects of the space environment on paint can dramatically alter the reflective properties of satellites. Although the solution set contains an almost infinite set of parameter combinations, it is reasonable to assume that, for any single given object, the physical features are sufficiently slowly varying such that, over a

reasonable observation time, the parameter solution space can be bounded. It is easy to see that appropriate characterization "fidelity" will depend on the "fidelity" of information contained in the data. In this analysis, we assume that space ageing effects and seasonal variations can be ignored, the latter affecting the phase angle geometry and thermal inputs. There are also time-dependent attributes associated with the attitude dynamics which can be manifested in the various measurements. The information content captured in the measurement model parameter statistics for each measurement type combine to paint a more complete picture of the dynamic and physical attributes.

For the four "states" (active, passive, dormant, transitory) being examined, the feature parameters are physically constrained by known material properties, sizes, shapes, the physics associated with the dynamics. One observation pass, which results in only a partial light curve of an object, is considered to be one observation sample. As the result of differing observation geometries exposing different surfaces at different orientations over different observing passes, photometric signature samples can look quite different from pass to pass. Examples of this are presented in the next section. We assume that the problem as stated is observable – the characteristic attributes can be extracted given a sufficiently large number of samples.

Given:

- Models of a 3-axis controlled satellite (INMARSAT used) and uncontrolled satellite (DiretTV-2 used).
- Multiple parameter signature models for: astrometric tracking, photometric, emissivity-area-product, temperature, and RF
- The physical/numerical constraints on these parameters.
- Gaussian statistical noise of the measurements (photometry, temperature, tracking, RF and emissivity-area-product).
- Sufficiently large sample sets of each measurement type to derive statistics indicative of a class of RSO as derived from the model parameters.

Determine:

- Parameterization models that capture the essential physical and dynamic attributes from the observation types (photometry, temperature, tracking, RF and emissivity-area-product).
- Probabilistic metrics that provide a measure for how likely one or more of a given measurement types is to be associated with an ensemble population of representative measurement metrics associated to a given RSO state (active, passive, dormant, transitory) as inferred from model parameter statistics derived from independent sets of measurements.

Two satellite models are used for simulation of the data used in this analysis. Figures 1 and 2 depict the INMARSAT and DirecTV-2 satellites, respectively. Previous work [3, 4] has addressed observational signatures from GEO satellites, including DirecTV-2, and so some of those models are leveraged in this work. In Section 4, techniques are derived for determining when a collection of observations are and are not associated with a unique object.

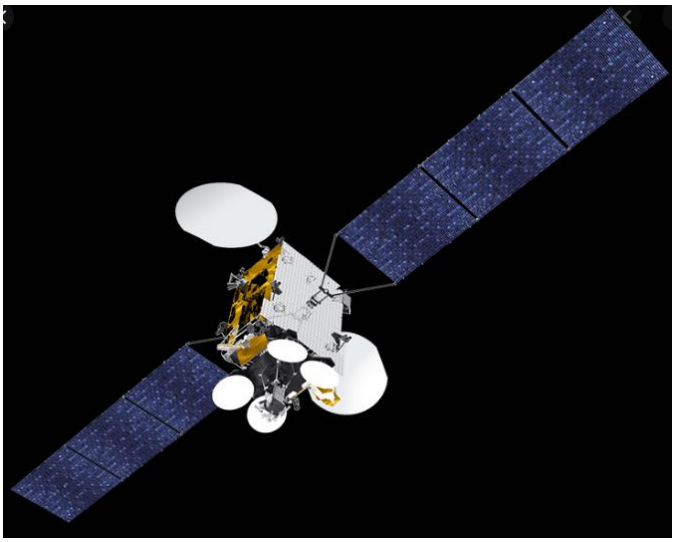

Figure 1. Active: INMARSAT satellite – used for active and transitory cases

Figure 2. DirecTV-2 satellite (Boeing 601 bus configuration) – used for passive and dormant cases

3. SIMULATED CASES

Simulated Right Ascension and Declination tracking data were derived from orbital dynamics for INMARSAT, a Geostationary satellite, and DirecTV-2 which is in a super-synchronous graveyard orbit and a hypothesized sensor located on Cyprus (e.g. the Starbrook sensor located at Geodetic Latitude = 34.91278° N, Longitude = 32.88389° E, Geodetic Altitude = 1773 m). Photometric, temperature, tracking, RF and emissivity-area-product data were simulated for several cases to demonstrate the application of information theory techniques towards addressing the association questions. Four cases representative of the four RSO state characteristics were simulated:

1) **Active**: 3-axis stabilized model of the INMARSAT satellite (box-wing) consisting of a bus, two solar array wings and 2 dish antennas,
2) **Passive**: an uncontrolled (tumbling) DirecTV-2 satellite consisting of a bus, two solar array wings and two dish antennas,
3) **Dormant**: the DirecTV-2 tumbling case but it periodically emits thermal and RF signatures, and
4) **Transitioning**: the 3-axis controlled INMARSAT box-wing model that becomes uncontrolled at some point over the observing span.

For all cases 200 light curve realizations (statistical samples) were generated over a 24 hour span and at a 30 second sampling interval. The process for simulating the data is depicted in Figure 3 where the initial position, velocity and attitude is specified at a given epoch, and propagated vs. time to support each of the measurement models used to generate photometric, emissivity-area-product, temperature tracking-rate and RF measurements. A single realization sample and composite of all sample set of realizations for State Cases 1) Active, 2) Passive, 3) Dormant and 4) Transitioning are shown in Figures 4, 5, 6 and 7, respectively, with representative noise added to the signals. Details for generation of the simulated data are provided in the following sections.

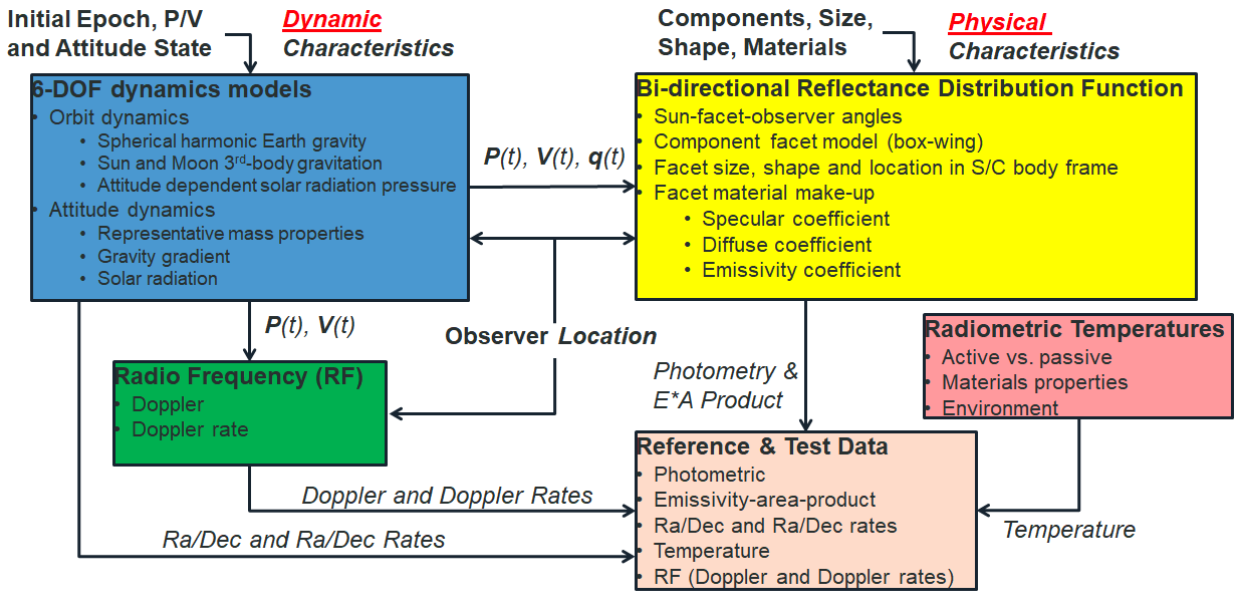

Figure 3. Simulated Data Generation Process

Simulated Photometric Measurements

The simulated photometric measurements were modeled as a function of the physical characteristics of the spacecraft, the position of the spacecraft, observation site, and sun using a Cook-Torrance BRDF model. The solar panels on the spacecraft are assumed to be facing the sun directly. The refelctivity of the entire spaceraft was determined through the combinatio of the solar panels, spacecraft bus, and two atennas illuminated by the sun and visible to the observer. The reflectivity of the components of the spacecraft was a combination of the diffuse and specular relfective components.

$$Reflectivity = SurfaceArea * \left(N \cdot r_{sun}^{body}\right) * \left(N \cdot r_{obs}^{body}\right) * \left(Ref_{diffuse} + Ref_{specular}\right) \quad (1)$$

Where N is the surface normal vector and the dot product with the sun body unit vector and the observer body unit vector. The diffuse and specular components are dependent on the associated material coefficients. This reflectivity calculation is repeated for all of the illumated and visible surfaces of the spacecraft. The reflectivity is then used to determine the visual magnitude of the spacecraft.

$$visualMagnitude = mag_{sun} - 2.5 \log\left(\frac{Reflectivity}{r_{obs}^2}\right) \quad (2)$$

Where $mag_{sun} = -27.26$ and is the r-band stellar magnitude. r_{obs} is the distance from the observer to the spacecraft. The visual magnitude of the satellite is calculated at each time step and has a $1-\sigma$ noise applied of 0.18 Mv. The simulation of the photometric measurements follows the same calculation for both INMARSAT and DirectTV, but the attitude, physical chararacteristics, and position of the satellites produce different results that are used in the analysis for object characterization.

Simulated Temperature Measurements

The temperatures measurements were modeld as a bias with both periodic and random (noise) components added for each of the simulated measurement trials. Representative values for active and passive (e.g. debris) RSO were derived from observational data collected by Skinner et al. [5, 6]. The mean temperature for the active, dormant and transitioning RSO's was taken to be 340° *K* each bias varying by a *1-σ* of 10° *K* and having a *1-σ* noise of 10° *K*, and an addition sinusoidal signature having an ampitude of 5° *K* and a period of 24 hours was also added. Similarly, the mean temperature for the passive RSO's was taken to be 300° *K* varying by a *1-σ* of 5° *K* and having a *1-σ* noise of

5° *K*, and the sinusoidal signature having an ampitude of 2° *K* and a period of 12 hours. All random components were generated from a Normal (Gaussian) distributions using the appropriate *1-σ* values.

Simulated Tracking-Rate Measurements

To simulate the tracking-rate measurements, first the Right Ascension and Declination were found at all of the individual timesteps. The Right Ascension and Declination measurements are the simulated astrometric products of an optical sensor image of the satellite. The optical measurements are only recorded when the RSO is illuminated by the sun and the ground observation site (Starbrook Sensor) is in darkness. The measurements are a function of the dynamics of the system, specifically the position of the satellite and the observation site. With the Right Ascension and Declination measurements, the tracking-rate measurements were derived and used to show a change in the Right Ascension and Declination which would be more effective in object characterization than the Right Ascension and Declination measurements. The tracking-rate measurements are useful to determine any change in the dynamics of the system, such as a maneuver. The Right Ascension and Declination measurements were simulated with the same process, orbital parameter dependent, for all states characterized.

Simulated RF Measurements

The Doppler shift is a phenomenon where the frequency of a signal measured by an observer shifts from the actual wave frequency due to the observer moving relative to the source of the wave. This is most apparent in everday occurences such as the shift in tone as an emergency vehicle passes by an observer. The shift or change in frequency (Δf) can be described using the following equation:

$$\Delta f = \frac{\Delta v}{c} f_0 \tag{3}$$

$$\Delta v = -(v_r - v_s) \tag{4}$$

Where c is the speed of the wave (which, in the case of an RF transmission, is the speed of light), f_0 is the frequency of the signal from the source, v_r is the velocity of the reciever and v_s is the velocity of the source.

The Doppler shift of an RF signal can be used to indicate the current active state of an RSO through the detection of a transmitted signal. An active or dormant RSO will periodically need to communicate to a groundstation for the transmission of satellite health data/commands etc. The presence of these RF signals can be detected and modelled using the Doppler shift as representative data of such a signal.

RF Dopper shift measurements were generated for each active state type using previously generated position and velocity data of the object as well as the Earth Centred Inertial position of the observer ground station (Starbrook Sensor). This is used for calculating the Δv in the Doppler shift equation. The active object type was modelled to continuously emit RF signals and therefor its doppler shift data is simulated for the full 24 hour span. A passive object is expected to have no RF signal emission. A transitioning object is modelled to have Doppler shift data simulated up to the point in time it transitions, indicating moving from an active transmitting object to a passive object no longer to transmit RF signals due to a failure for example. Finally, the case where a dormant object is occasionally transmitting RF signals has been modelled to include 3 randomly selected periods of time during the 24 hour timespan where the predicted Dopppler shift is modelled for 1 hour for each period. The frequency assumed for the downlink transmission is approximately 1525Mhz.

Simulated Emissivity-Area-Product Measurements

The simulated emissivity-area-product measurements are a product of LWIR measurements of an RSO. It is a dunction of thethermal radiation and the projected area of the RSO. Skinner, et al. describe the emissivity-area-product as the ratio of the gray body thermal radiation to the black body thermal radiation times the projected area of the object. In other words, it is a measure of the self-emitting thermal signature of an object, which can be used to characterize an object [5, 6]. Similar to the simulated photometric measurements, only the components of the spacecraft that are illuminated by the sun and visible to the observer were considered. The emissivity-area-product can be determined by the following equation:

$$EAP_{surface} = SurfaceEmissivityCoefficient * SurfaceArea * \left(N \cdot r_{obs}^{body}\right) \quad (5)$$

The emissivity-area-product is calculated for all of the observable surfaces and the sum of the emissivity-area-products of all the surfaces equals the total emissivity-area-product of the RSO. The emissivity-area-product is calculated at each timestep and has a $1-\sigma$ noise of 0.5 m^2 applied. For each of the characterization states, the emissivity-area-product was calculated using the above equations. Similar to the photometric measurements, the emissivity-area-product gives insight to the stability of the spacecraft for object characterization.

Below shows the five measurement types for the four different classifaction types.

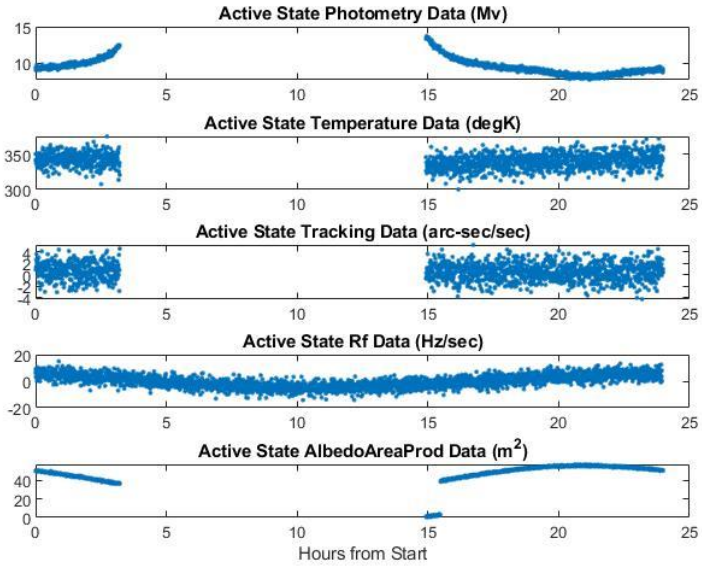

Figure 4. Active mon-maneuvering: INMARSAT 3-axis stabilized box-wing model

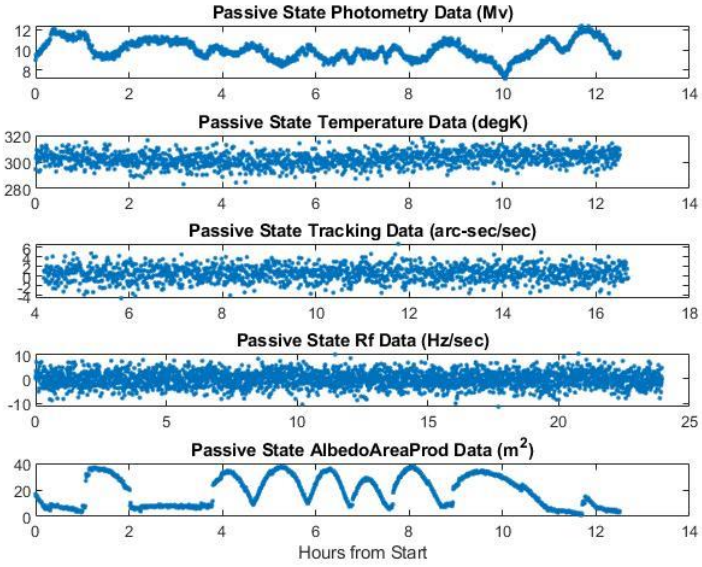

Figure 5. Passive: DirecTV-2 un-controlled (tumbling) box-wing model

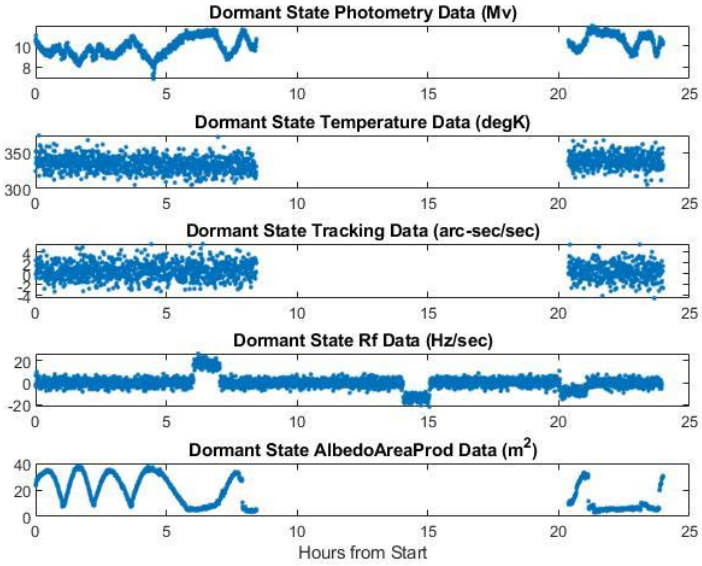

Figure 6. Dormant non-maneuvering: DirecTV-2 un-controlled (tumbling) box-wing model with periodic thermal and RF emissions

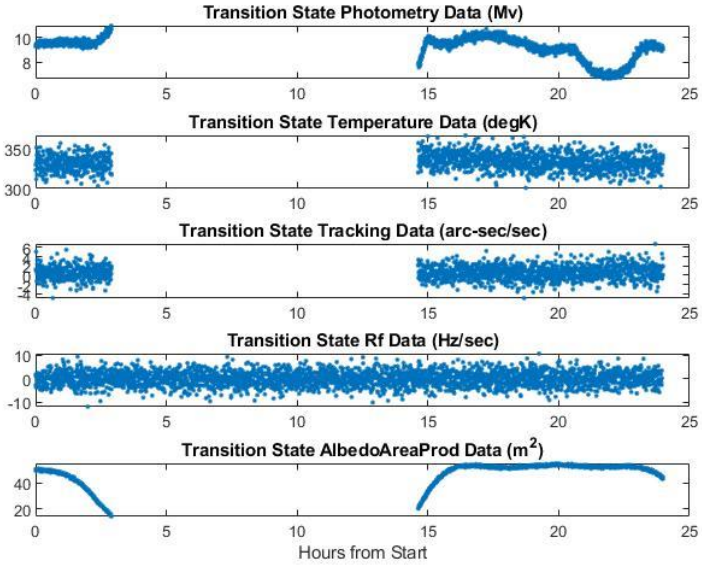

Figure 7. Transitioning: INMARSAT 3-axis stabilized box-wing model that goes from 3-axis controlled to uncontrolled

As the four cases illustrate, each measurement type can be represented by a time history of observations consisting of a characteristic signature combined with both systematic and random errors resulting from imperfections intrinsic to the observing system, environment and geometry. The signature itself is of interest as its variations over time and geometry reveal the physical and dynamic attributes of the unresolved object. In the next section of this paper an alternative representation of the light curve that is more conducive to exploring the information content is presented and, provides an analytical tool for associating independent set of observations with no *a priori* association knowledge. The simulated test data sets are used to test these information-based techniques to show they can appropriately classify like attributes as well as provide indicators that selected light curve comparisons form different RSO states.

4. APPLICATION AND ANALYSIS OF INFORMATION THEORY TECHNIQUES

4.1. Mathematical and Probabilistic Motivation

A measurement time history can be mathematically represented as functions in order to use information theory to provide a rigorous probabilistic analysis of measurement phenomenon. This approach differs from the conventional approach that treats measurements as a point-wise time series sequence of points. A measurement at time t over a time interval of length T is denoted by Z_t^T, object characteristic parameters by x_t, and geometric parameters by g_t. Only Z is treated as a curve (or model) over the interval T, while the state and geometric parameters are assumed to be represented in a holistic way based on the state of the object and geometric parameters over the window of time T. For example, the state x represents the spin state of the satellite over the interval T, including the possibility that it is executing a complex attitude motion. A joint distribution on these parameters is denoted by $p(Z_t, x_t, g_t)$ (for ease of notation, the superscript T is dropped). Along with the joint distribution, data models (e.g. *BRDF* model for light curve models) are used to compute the likelihood $p(Z_t|x_t, g_t)$. This was used in a pointwise (i.e., not as a function) context of Multiple Adaptive Model Estimation (MMAE) in [2]. The probabilistic framework utilized in this paper enables a rigorous Bayesian analysis, where the posterior characteristic associated with the object state can be computed given the observation and geometry parameters $p(x_t|Z_t, g_t)$ or the joint posterior in both object state and geometric parameters given an observation $p(x_t, g_t|Z_t)$. This treatment, which assumed a single measurement type, can be expanded to include multiple but independent measurement types.

To probabilistically analyze multiple sets of measurement time series, tools from Functional Data Analysis (FDA) [7, 8] are used. Such an approach has been used in genetic analysis [9] and star and planetary classification based on an FDA analysis of light curves [10]. In fact, this work expands on Kelecy et al. [1] which demonstrated the use of FDA for characterizing states using light curves. In FDA, a curve is converted into a finite-dimensional vector using an appropriate basis system that guarantees capturing of the main features of a light curve signal. In general, the functional representation can be expanded to multiple dimensions to accommodate multiple independent measurement types. From there on, any result that is established for finite dimensional spaces can now be applied to multi-dimensional functional data. Reference [11] uses the Mahalanobis distance to process functional data for classification.

In addition to a rigorous Bayesian approach to light curve analysis, information theory can address many space situational awareness (SSA) problems. One can compute information divergence between two classes of light curve data to assess how much common information exists between the two sets of data. Such an analysis can reveal, for example, that two objects share one or more common facets. Another example is to use mutual information to solve the object-to-object correlation problem by assessing how much information overlaps between two observed objects with two light curves collected at different time instances. The proposed FDA-based probabilistic viewpoint enables the replication of many of the information theoretic results developed for angles and/or range observations [12, 13] for light curves processing.

If we define a "measurement state" $x(t)$ as a function of time *t*, then for measurements of type *z* we can define *n* sets of measurements M_z over a sequence of *m* time-tags as

$$M_z = \{x_i(t_{ij}) : i = 1, \dots, n \; and \; j = 1, \dots, m\} \tag{6}$$

where $x_i(t_{ij})$ is the a measurement in set *i* at the time instant *j*. If we assume that the measurements can be represented by a linear functional form in terms of basis functions $\varphi_k(t_{ij})$ and coefficients β_{ik} then

$$x_i(t_{ij}) \cong \sum_{k=1}^{K} \beta_{ik} \, \varphi_k(t_{ij}) \tag{7}$$

where *K* is the number of basis functions that adequately represent the measurements. The functional sample mean and covariance for the collection of measurements for a given type are then computed as

$$\hat{\mu}_x = \frac{1}{n} \sum_{i=1}^{n} \beta_i \, (t_{ij}) \tag{8}$$

and

$$\widehat{\Gamma_x} = \frac{1}{n}\sum_{i=1}^{n}(\beta_i - \hat{\mu}_x)^T\,(\beta_i - \hat{\mu}_x) \tag{9}$$

It should be noted that the functional formulation removes the time-dependence and instead captures the statistical characteristics represented by the functional parameters β_{ik}. The previous work [1] showed the potential for ambiguous characterization results due to geometric and dynamic conditions that resulted in similar light curve characteristics. For example, a cube spinning about an axis that is aligned with the observer might look like a 3-axis stabilized cube with the reflected light from the surface of the spinning cube does not vary with time as would be the case for the 3-axis stabilized cube. The value of multiple measurement types is the potential for providing additional information associated with different physical attributes that the ambiguous measurements do not provide.

4.2. Computing Likelihood of a Measurement Phenomenon

The next question we address in this paper is: How can one determine the likelihood that a measurement time history was generated by an RSO with previously classified characteristics? Given a candidate RSO's dynamics, shape type, the type's first and second moment statistics are obtained as described in the last subsection. Those results suggest that the Mahalanobis type of distance metric can be used to assess whether the measurement sequence belongs to one of the available measurement classes [11]. This analysis enables the determination of whether a new measurement sequence belongs to a specific family of measurements associated with a specific class of RSO (e.g. active, passive, dormant or transitory). It shows commonality of features between the new measurement sequence and ones in the family. These results also enable use of the divergence metrics, for example, to determine the degree of commonality between two classes of measurement populations. For this work, we introduce the use of a normalized distance metric which enables the combination of multiple distance measurements for each measurement type: The Hellinger Distance which is related to the Bhattacharyya divergence [14]. The Bhattacharyya divergence between two probability distribution functions (pdfs) *p(x)* and *q(x)* is given by:

$$D_B(p||q) = -\log\big(B_C(p||q)\big) \tag{10}$$

where B_c is the Bhattacharyya coefficient and is given by

$$B_C(p||q) = \int \sqrt{p(x)q(x)}dx \tag{11}$$

Note that $0 \le B_C(p||q) \le 1$ and $0 \le D_B(p||q) \le \infty$, and so does not obey the triangle inequality. If both p and q are assumed to be Gaussian, then one can compute $D_B(p||q)$ in closed form which is derived as:

$$D_B(p||q) = \frac{1}{8}\big(\mu_p - \mu_q\big)^T\Gamma^{-1}\big(\mu_p - \mu_q\big) + \frac{1}{2}\log\left(\frac{\|\Gamma\|}{\sqrt{\|\Gamma_p\|\|\Gamma_q\|}}\right) \tag{12}$$

where μ_p and Σ_p, and μ_q and Σ_q, are the mean and covariance of the distributions p and q, $\|.\|$ denotes the determinant of the given covariance, and

$$\Gamma = \frac{1}{2}\big(\Gamma_p + \Gamma_q\big) \tag{13}$$

The Bhattacharyya coefficient is related to the Hellinger distance D_H as:

$$D_H(p||q) = \sqrt{1 - B_C(p||q)} \tag{14}$$

where $D_B(p||q)$ is derived from equation (7) (assuming Gaussian distributions) and

$$B_C(p||q) = e^{-D_B(p||q)} \tag{15}$$

The Hellinger distance is a proper divergence metric because it satisfies the non-negativity, symmetry and triangle inequality properties. This metric is used in the subsequent analysis to determine the "compatibility" of distributions of a set of one or more measurement types on a given RSO with the distribution metrics derived for an RSO with established distribution characteristics for those same measurement types. It is a measure of how one probability distribution is different from a second, reference probability distribution, where a divergence of 1 indicates that the two distributions in question are identical and at the opposite extreme a value of 0 indicates they are substantially different. If $D_H^j(p_j||q_j)$ represents the Hellinger Distance between distributions p_j and q_j for measurement types j = *1, 2, …, N*, then when considering the compatibility of distributions associated with multiple measurement types the combined distance metric can be computing by the Root Mean Square (RMS) as

$$D_H = \sqrt{\sum_{j=1}^{N}\left[D_H^j(p_j||q_j)\right]^2/N} \tag{16}$$

This fusion of the Hellinger Distance metric for various combinations of measurements represents a combined likelihood of a given "test" measurement set being associated with a previously established set of statistics "trained" on a pre-established set of labelled data representing a state class. A value of D_H closer to zero indicates a close ("good") comparison between distributions whereas a value closer to one points to dissimilar ("poor") comparison.

5. INFORMATION ASSESSMENT VS. MEASUREMENT COMBINATIONS

The data for each case were analyzed using the Hellinger Distance metric in the following way. Each data set was split into two parts where half was used to establish a "Reference" set of classification statistics and the second half was used as a test data set for each state. The reference data was fit to a high order polynomial, as an example of a parameterized measurement model, and the mean and covariance of the polynomials was computed. A likelihood function was then generated by evaluating the second half of each realization to the sample functional mean and covariance, assuming a Gaussian distribution. This approach insured independent data sets were used for computation of the mean and covariance versus the "test samples" used for evaluation of the likelihood. In this exercise, the polynomial order used was dependent on the measurement type:

Measurement – Polynomial Order

- Photometry – 10
- Temperature – 2
- Tracking rate – 0
- RF – 3
- Emissivity-area-product – 10

A more in-depth analysis should be done to evaluate appropriate orders, and even different parameterization models. The model should retain the "signal" of interest (information) while minimizing noise and error related artifacts. Since the Hellinger metric is a measure of "distance", or comparability, between two distributions, a lower number closer to "zero" indicates that the distributions are similar where as a value closer to "one" indicates they are different.

Figures 8, 9, 10, 11 and 12 show the Hellinger distance metrics for the "Test" vs. "Reference" data for each of the four states and for photometric, temperature, tracking rate, RF and emissivity-area-product, respectively. In each of the figures the color and value in each square represents the Hellinger Distances computed from the data sets for one of the four given "Test" states versus one of the four given "Reference" states. Again, the lower (blue) numbers indicate a good comparison between the computed distributions whereas the larger (red) numbers indicate poor comparison. Note, the number/color scales differ for each of the plot but the previous comparison guidelines hold. Results for each measurement type are summarized as follows:

- Photometry: The photometry only results shown in Figure 8 indicate that all four test states match well (small Hellinger metric) with their corresponding reference states. However, the dormant and passive states prove ambiguous due to the similarities between their photometric signatures. There is no way to distinguish dormant from passive based upon photometry alone.

- Temperature: Similarly, the temperature comparisons in Figure 9 show successful association between test and reference states, but are ambiguous between active, dormant and transitioning due to similarities in the temperature profiles which assumes similar characteristics due to thermal conditioning (heated sensors).
- Tracking rate: The tracking rate comparisons shown in Figure 10 are by and large completely ambiguous due to only slight differences between the geosynchronous and supersynchronous rates. Perhaps inclusion of the declination components and/or other higher order tracking metrics would provide a greater distinction. Incorporation of maneuver signatures into the right ascension rate metrics is currently being explored. Additionally, including more measurement diversity in the samples to prevent geosynchronous satellites being exclusively characterized as active/transitioning and supersynchronous satellites being exclusively categorized as passive/dormant due to limited measurement diversity. This is also currently being explored through the inclusion of maneuvers in the data which would appear in the tracking-rate measurements. Maneuvers would be a characteristics for active and dormant satellites, which could be another way to disambiguate the different states.
- RF rate: The RF (Doppler Rate) comparisons presented in Figure 11 show decent comparisons between test and reference states in all cases, but also show some ambiguity between passive and transitioning due to loss of signal in the transition case which goes from active to passive (no RF transmission). The higher correlation between Passive and Transition is due to an RF signature which occurs at the beginning of the Transition data while the RSO is still 3-axis stabilized and Active.
- Emissivity-area-product: The emissivity area product comparisons in Figure 12 are similar to the photometry (Figure 8) due to the similarities in their signatures resulting in ambiguity between passive and dormant.
- Root-mean-square: The Hellinger Distance comparisons computed through the RMS combination of all measurements, presented in Figure 13, demonstrate unambiguous state characterization as the combination of contained in each measurement type contributes unique information which eliminates the ambiguity. Similarities in temperature and RF signals result in lower metrics for Active-Dormant state comparisons. Photometric and Emissivity-area-product similarities also result in lower metrics for the Passive-Dormant comparisons.

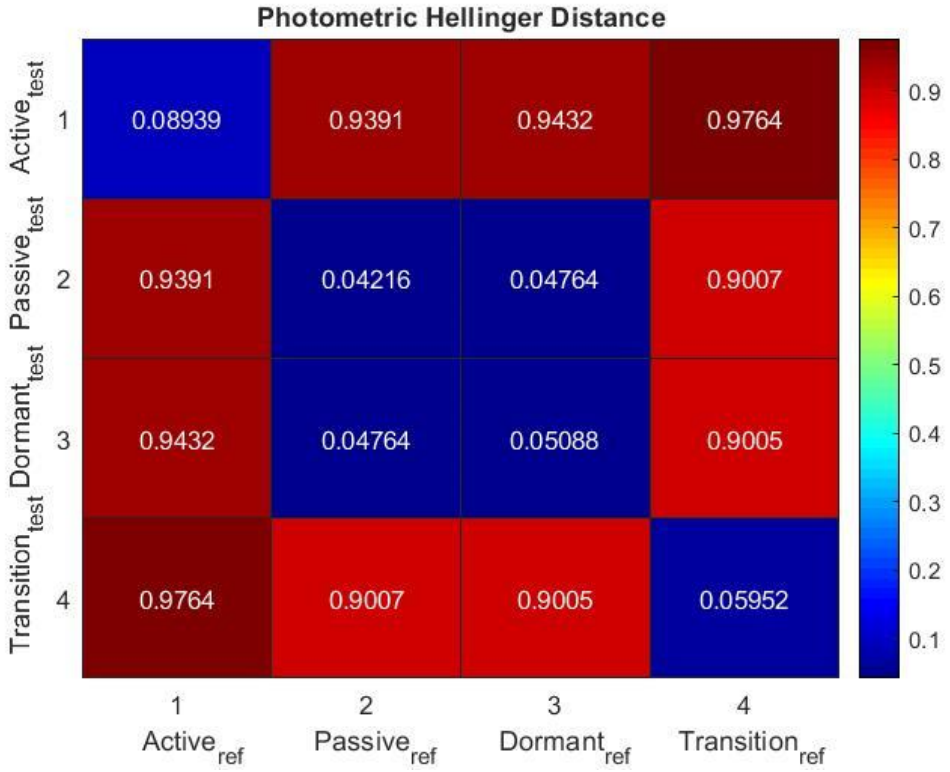

Figure 8. Photometric Hellinger Distance Metrics vs. State

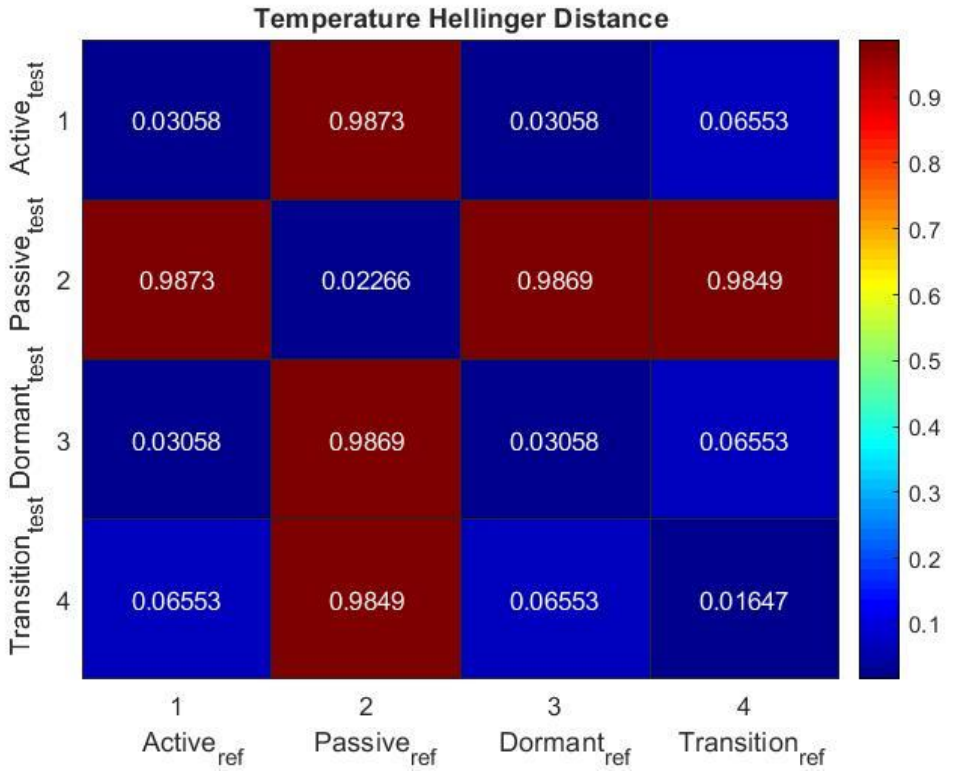

Figure 9. Temperature Hellinger Distance Metrics vs. State

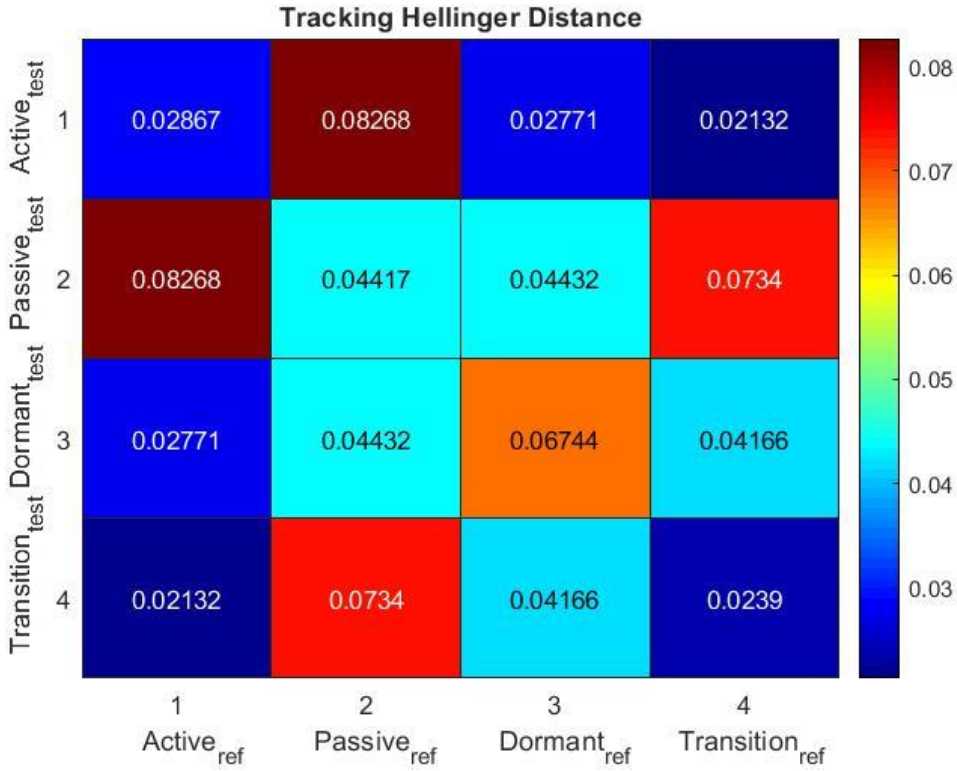

Figure 10. Tracking Rate Hellinger Distance Metrics vs. State

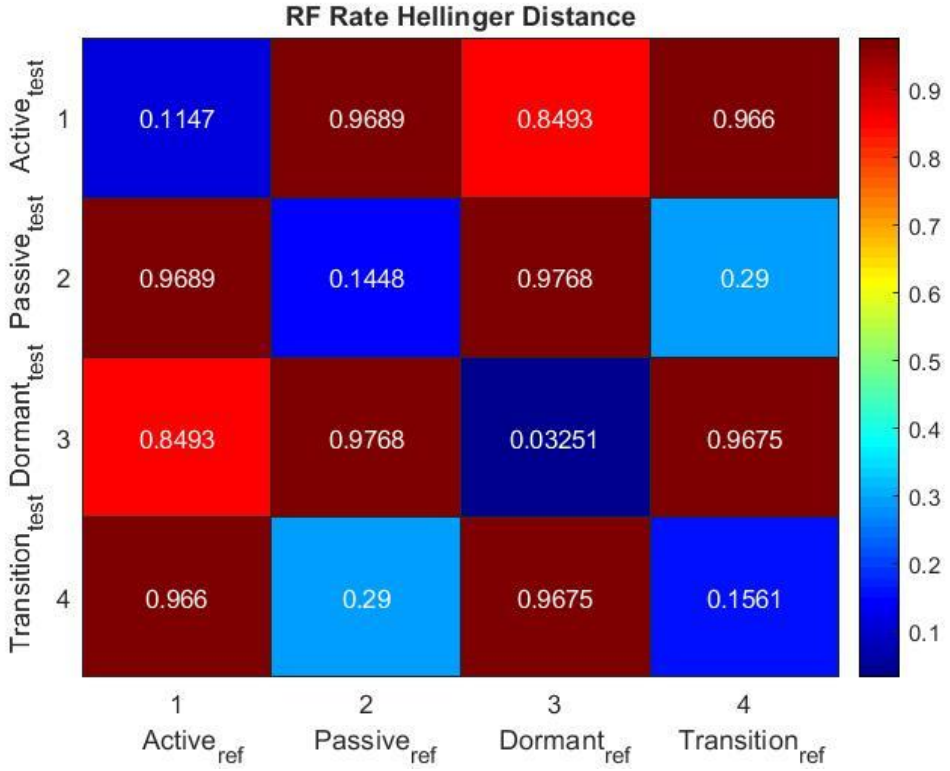

Figure 11. RF Hellinger Distance Metrics vs. State

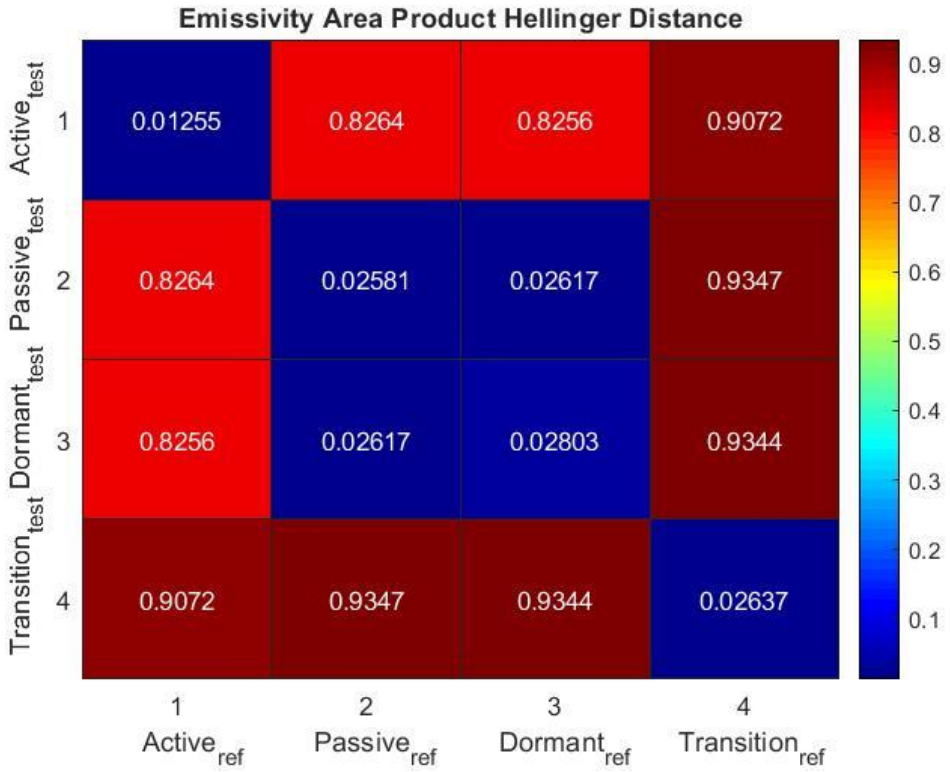

Figure 12. Emissivity-area-product Hellinger Distance Metrics vs. State

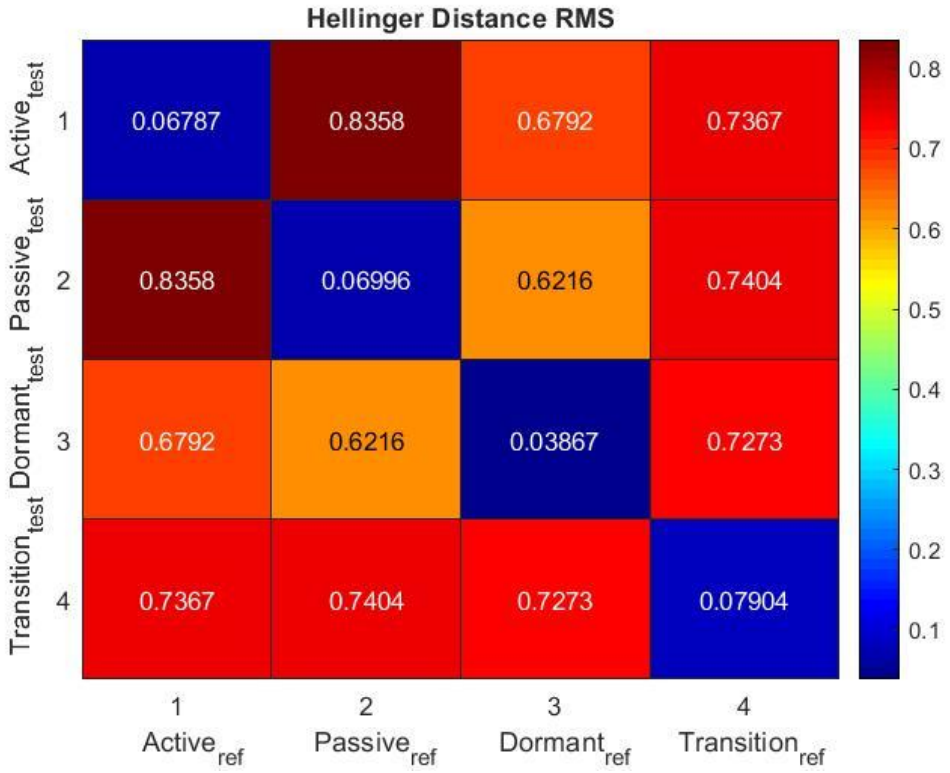

Figure 13. RMS (all measurements) Hellinger Distance Metrics vs. State

6. CONCLUSIONS

Previous results showed the potential for ambiguities in the characterization when only photometric data were available [1]. These analysis results for diverse measurements representative of the four activity states demonstrates the viability of applying probabilistic functional data analysis approach to characterizing the "true" state based on fusion of the multiple measurement types. Using FDA, a combined Hellinger Distance metric was derived and shown to result in a high degree of successful characterization without ambiguities when multiple measurement types were included. Similarly, these results also showed a low likelihood of a set of realizations from one RSO state being associated with a distribution derived from a different RSO state. Though this makes intuitive sense, these results not only quantify the value of multi-data fusion in characterization, but it sets up the ability to gauge the value of specific information that each measurement type contributes to each class. The population of measurements for a given RSO state retain a unique information content that allows these approaches to be successfully applied via the Hellinger Distance metric. The information theoretic metrics provide a measure of how well the association can be quantified and, hence, a measure that can be used to prioritize tasking of subsequent observations to reduce ambiguity and increase the probability that a set of signatures belong to the same object. Lastly, the FDA technique can be used to characterize any "attribute" whose signature can be captured in data which can modeled and used as a reference.

Future analysis will be conducted to include the following analyses:

- Looking at how many samples are needed for reliable results
- Assumptions on Gaussian vs. other distributions in distance metrics
- Examination of other classification categories vs. additional data types
- More thorough assessment of value of each data type
- Looking at other models vs. polynomial
- Examining sensitivity to maneuvering vs. non-maneuvering RSOs

Real measurement data will also be analyzed to further validate these results.

7. ACKNOWLEDGEMENTS

We would like to thank the Air Force Office of Scientific Research (AFOSR), and in particular Mr. Kent Miller (now retired), for funding this work. We would also like to thank Dr. Weston Faber for his suggestion to use the Hellinger Distance as a characterization performance metric. It was appropriate and worked well.

8. REFERENCES

1. Kelecy, T., I. Hussein, K. Miller and J. Coughlin, "Probabilistic Analysis of Light Curves," Journal of the American Astronautical Society, ORCID ID 0000-0003-3958-6419, May 2018.
2. Linaris, R., Jah, M. K., Crassidis, J., Nebelecky, C.: Space Object Shape Characterization and Tracking Using Light Curve and Angles Data. Journal of Guidance Control and Dynamics, Vol. 37, No. 1, pp. 13-25, January (2014).
3. Skinner, M., R. Russell, T. Kelecy, S. Gregory, R. Rudy, D. Kim and K. Crawford, "Observations in the thermal IR and visible of a retired satellite in the graveyard orbit, and comparisons to active satellites in GEO," Acta Astronautica, 105 (2014) 1-10, Elsevier ScienceDirect, August 2014.
4. Skinner, M., R. Russel, T. Kelecy, S/ Gregory, R. Rudy and D. Kim, "Comparison of Thermal IR and Visible Signatures of Graveyard Orbit Objects," 66th International Astronautical Congress, (IAC-15-A6.1.4) Jerusalem Israel, 2015.
5. Skinner, M., R. Russell, R. Rudy and D. Kim, "Broadband Array Spectrograph System (BASS) thermal IR observations of Low Earth Orbit (LEO) and Geosynchronous Earth Orbit (GEO) objects in sunlit and darkness conditions," 68th International Astronautical Congress, (IAC-17-A6.1.6) Adelaide, Australia, 2017.
6. Skinner, M., R. Russell, R. Rudy and D. Kim, "Utilization of Broadband Array Spectrograph System (BASS) thermal IR observations of geosynchronous earth orbit (GEO) objects in the creation of an observation-based model of their thermal emission," 69th International Astronautical Congress, (IAC-18-A6.1.5) Bremen, Germany, 2018.
7. Gine, E., Nickl, R.: Mathematical Foundations of Infinite-Dimensional Statistical Models. Cambridge Series in Statistical and Probabilistic Mathematics (2015).
8. Wang, J. L., Chiou, J. M., Muller, H. G.: Review of functional data analysis. Annual Review of Statistics and Its Application, Vol. 3, pp 257-295 (2016).
9. Leng, X., Müller, H. G.: Classification using functional data analysis for temporal gene expression data. Bioinformatics, 22 (1): 68-76 (2006).
10. Faraway J., Mahabal, A., Sun, J., Wang, X.-F., Wang, Y. G., Zhang, L.: Modeling light curves for improved classification of astronomical objects. Statistical Analysis and Data Mining, Vol. 9, pp. 1–11 (2016).
11. Galeano, P., Joseph, E., Lillo, R. E.: The Mahalanobis Distance for Functional Data with Applications to Classification. Technometrics, Vol. 57, No. 2, pp. 281-291 (2015).
12. Hussein, I., Wilkins, M. P., Roscoe, C. W. T., Schumacher, Jr., P. W.: On Mutual Information for Observation-to-Observation Association. 25th AAS/AIAA Space Flight Mechanics Meeting, Williamsburg, VA, January 11–15 (2015).
13. Hussein, I., Roscoe, C. W. T., Schumacher, Jr., P. W., Wilkins, M. P.: UCT Correlation using the Bhattacharyya Divergence. Proceedings of the 26th AAS/AIAA Space Flight Mechanics Meeting, Napa, CA, February 14–18 (2016).
14. Hussein, I., C. Roscoe, M. Wilkins and P. Schumacher, "Track-to-Track Association Using Bhattacharyya Divergence," Proceedings of the 16th AMOS Technical Conference, Wailea, HI, 2015.